MCM-41 silica monoliths with independent control of meso- and macroporosity

Jérôme Babin,[a] Julien Iapichella,[a] Benoît Lefèvre,[a] Christine Biolley,[a] Jean-Pierre Bellat,[b] François Fajula[a] and Anne Galarneau*[a]

Received (in Montpellier, France) 27th July 2007, Accepted 13th September 2007
First published as an Advance Article on the web 10th October 2007
DOI: 10.1039/b711544j

Centimetre sized macroporous silica monoliths consisting of MCM-41 have been prepared by a two-step procedure allowing an independent control of the meso- and macro-porosity. In the first step a monolith with a macroporosity tailored between 2 and 20 μm is prepared under acidic medium by a phase separation, named spinodal decomposition, leading to a bicontinuous structure of a silica/polymer phase and a water phase. The monolith is then reacted in an alkaline solution of cetyltrimethyl ammonium to transform the silica skeleton into MCM-41 under conditions which preserve the original morphology and macroporosity of the material. The combination of spinodal decomposition and pseudomorphic transformation proves very efficient to precisely tune the textural characteristics of macroscopic objects.

Introduction

Cooperative self-assembly between organic surfactant micelles and inorganic species, such as silica,[1–3] is a powerful tool for producing stable ordered mesoporous materials, characterized by extremely narrow pore size distribution, high specific surface area and large pore volume.[4–7] Thanks to these unique textural properties, mesoporous materials have attracted great attention, over the past decade, in wide research areas that include catalysis,[8,9] biocatalysis,[10,11] separation, optics,[12] sensor, drug delivery[13] and so on. Moreover, with the progress in the synthesis of micelle-templated silica (MTS) materials, different macroscopic shapes are now accessible such as fine powders, fibers, thin films and monoliths.

The incorporation of mesoporous monoliths into operational devices (chromatographic columns, catalytic reactors...) entails the presence of a hierarchical porosity (macropores/mesopores) to allow efficient and rapid mass transport through the material with a minimal operating pressure while optimizing the mass to volume ratio. Mesoporous monoliths with a continuous network of macropores constitute the best candidates for such applications.

To date, three ways are known to produce monolithic silicas with well defined continuous macropore networks. The first one is the nanocasting method where large structure-directing agents, like polymeric colloids[14–17] or resins,[18] (micro)emulsions,[19] gas foams[20] and starch gel,[21] are used as macroporogenes during a sol–gel process.

A second method, introduced by Nakanishi in 1992,[22,23] is based on concurrent phase separation and gelation processes occurring in acidic media during a hydrolytic sol–gel synthesis of silicon alkoxide precursors, in the presence of additives like organic polymers. Here, the phase separation through a spinodal decomposition mechanism (which occurs in the unstable region of the miscibility window) is induced by both the polymerization of the alkoxysilane (decrease of the mixing entropy) and the unfavourable interaction between water and the silica in formation surrounded by polymer (increase of the mixing enthalpy). The resulting transitional structure formed by bicontinuous silica-rich and water-rich phases is then fixed by the sol–gel transition and leads, after removal of the liquid phase, to the macroporosity. Kinetic control of both the phase separation and the gelation, obtained through the composition of the starting mixture and the temperature of the synthesis, allows one to tune both the diameter of the macropores and the size of the skeletons between 1 and 50 μm.[22] After this first step, the skeleton of the monoliths is microporous and weakly condensed, and therefore exhibits low mechanical stability.

Higher stability and disordered mesopores can be generated in the skeleton of the monolith by a second post-gelation treatment in mildly basic solution (ammoniacal solution or *in situ* urea decomposition) involving Ostwald ripening inside the silica skeleton to produce interparticular mesoporosity together with silica condensation.[24] The size of this disordered mesoporosity is controlled by the temperature of the treatment and the basicity of the solution. Mesopores from 6 to 30 nm have been tuned for post-gelation temperatures in ammoniacal solution from 40 to 150 °C, respectively, leading however to a decrease of surface area from 800 to 100 $m^2\ g^{-1}$ due to the increase of size of the elementary nanoparticles.[25]

Finally, the use of glycol-modified silanes,[26] of triblock copolymer surfactants, such as poly(ethylene oxide)-*block*-poly(propylene oxide)-*block*-poly(ethylene oxide), named P123[27,28] ($PEO_{20}PPO_{70}PEO_{20}$) and F127[29] ($PEO_{106}PPO_{70}PEO_{106}$), as water soluble polymers instead of PEO or the incorporation of cetyltrimethylammonium bromide[30] (CTAB) surfactant in addition to PEO during the first step of the phase

[a] *Institut Charles Gerhardt Montpellier-UMR 5253 CNRS/ENSCM/Matériaux Avancés pour la Catalyse et la Santé, Ecole Nationale Supérieure de Chimie de Montpellier, 8 rue de l'Ecole Normale, 34296 Montpellier Cedex 5, France. E-mail: anne.galarneau@enscm.fr*
[b] *Institut Carnot de Bourgogne, UMR 5209 CNRS, Université de Bourgogne, 9 A. Savary, BP 47870, 21078 Dijon, France*

separation has been proposed to obtain, in one single step, monolithic silicas with a hierarchical organisation of macro- and periodically arranged mesopores. However, because the phase separation process is highly sensitive to the composition of the medium, the interconnected macropores and the ordered mesopores could not be controlled independently and in any case small macropores, around 1 μm or less in size, were obtained. P123 alone instead of PEO features uniform interconnected macropores of 0.4 μm and a low ordering in mesoporosity. The addition of a precise amount of 1,3,5-trimethylbenzene (TMB) allows one to obtain a well-ordered hexagonal mesoporosity of 6 nm pores with a macroporosity of 0.6 μm featuring a less uniform skeleton than with P123 alone.[26,27] The addition of CTAB to PEO[30] leads to a drastic decrease of the size of the macropores compared with those obtained with PEO only, and a low level of organization of the mesopores was obtained as confirmed by the absence of small angle X-ray scattering signals. Furthermore, as solvent exchange was necessary to increase the stability of the silica gels before drying, an additional textural mesoporosity was always present in the monolithic samples, leading to trimodal porosity.[30]

In the present work, we have successfully combined the Nakanishi synthesis procedure for gaining macroporosity control and the secondary pseudomorphic synthesis recently developed in our group[31,32] for producing ordered mesoporosity in the skeletons. Monolithic silicas with a bimodal organisation of macropores and periodically arranged mesopores of MCM-41 type inside the skeleton have been then produced. Unlike previous studies, this new approach allows the independent control of the macro- and mesopore properties and also avoids the presence of additional textural mesoporosity.

Experimental section

Materials synthesis

The silica monoliths were synthesized using tetraethoxysilane (TEOS), polyethylene oxides of different molecular mass: PEO-10000, PEO-35000, PEO-100000 (with molecular mass = 10 000, 35 000, 100 000 g mol^{-1}, respectively), cetyltrimethylammonium bromide (CTAB) purchased from Aldrich, and aqueous NH_4OH (analytical grade), NaOH and HNO_3 (70%) obtained from SDS.

Preparation of monolithic silicas with disordered mesoporosity

The silica gel mixture was prepared following the procedure described by Nakanishi.[22,23] In a typical synthesis (M2), 1.690 g PEO-10000 was added to 16 g of water and 1.37 g of HNO_3 (70%). The solution was cooled in an ice bath and was stirred until complete dissolution of the polymer. Then 12.62 g of TEOS was added and the mixture was stirred vigorously in the ice bath for 30 min. The molar composition of the sol is then: 1 TEOS–14.8 H_2O–0.25 HNO_3 with a molar ratio of ethylene oxide unit per silica of EO/Si = 0.64. The resultant transparent solution was poured into hydrophobized (with $(CH_3)_2SiCl_2$) glass tubes or plastic tubes (straw or PVC tubes) of 10 or 5 mm internal diameter and 8 cm length closed by two laboratory films at room temperature and allowed to gel at 40 °C for 3 days in a water bath. After 2 h at 40 °C, the solution became turbid, then transformed into a gel with a transparent supernatant constituted of ethanol coming from TEOS hydrolysis. A 1–2 mm shrinkage occurs upon gelation allowing easy removal of the silica monoliths from their molds. The monoliths were then put in a water bath for 4 days to neutralize the excess acid. At the end of this first stage, silica monoliths present well-defined co-continuous macropores as a result of concurrent phase separation and sol–gel transition induced by the polymerization reaction, whereas the silica skeleton is weakly condensed and exhibits only a microporosity after drying and calcinations.[25] In the Nakanishi synthesis procedure, a second step in basic medium is applied to generate a disordered mesoporosity by a dissolution–reprecipitation process of the silica network and Ostwald ripening. The wet silica monoliths obtained in the first step are transferred to a 125 mL autoclave and immersed in 70 mL of a 0.1–1 M NH_4OH aqueous solution (different NH_4OH concentrations induce different sizes of mesopores). The hydrothermal temperature was raised to 80 °C and the reaction time was 24 h. The monoliths were rapidly rinsed with water and dried in an oven at 40 °C on a flat surface for 2 days. The monoliths were then calcined at 550 °C for 8 h under air flow to remove the remaining PEO.

The protocol detailed above using PEO-10000 leads to monoliths with macropores of 2 μm in size as determined by SEM. The monoliths of this family will be identified as M2 monoliths. To obtain larger macropore sizes (with pores of 10, 15 and 20 μm size, hereafter identified as M10, M15 and M20, respectively), PEO with higher molecular weights (M_w = 35 000, 100 000 g mol^{-1}) or different composition ratios were used. Experimental conditions are summarized in Table 1.

Preparation of silica monoliths with ordered mesoporosity of MCM-41 type

Silica monoliths obtained after the bi-continuous phase separation in acidic media (as previously described), *i.e.* after the formation of the macroporous network, were subsequently reacted in an alkaline solution containing CTAB, NaOH and H_2O. Different reaction mixtures of the three components

Table 1 Experimental data for the synthesis of silica monoliths with different macroporosity and disordered mesoporosity

Sample	PEO M_w/g mol^{-1}	Macroporosity (SEM)/μm	TEOS (mol)	H_2O (mol)	HNO_3 (mol)	EO/Si	NH_4OH concn/M
M2	10 000	2	1	14.8	0.25	0.64	0.1
M10	35 000	10	1	14.64	0.9	0.593	0.5
M15	35 000	15[a]	1	14.64	0.9	0.58	1.0
M20	100 000	20	1	14.7	0.25	0.63	0.1

[a] Plus cavities 1 μm (see text).

Table 2 Porosity (macro- and mesoporosity) features of monoliths after treatment with ammonia (concn in Table 1) determined by SEM, Hg porosimetry and nitrogen sorption at 77 K

Sample	$D_{SEM(macro)}$/m	$D_{Hg(macro)}$/m	$V_{Hg(macro)}$/L g^{-1}	$D_{Hg(mes)}$/nm	$V_{Hg(mes)}$/mL g^{-1}	$D_{N2(mes)}$/nm	$V_{N2(mes)}$/mL g^{-1}	S_{BET}/m^2 g^{-1}
M2	2	1.2	2.13	14.5	1.05	20.1	1.13	417
M10	10	5.1	1.77	10.1	1.03	26.0	1.26	251
M15	15	8.8	1.90 (0.35)[a]	16.9	1.00[b]	28.0	1.09	211
M20	20	16	2.10	15(?)	1.15	18.6	1.17	500

[a] Pore volume of the 1 μm cavities. [b] Mesopore volume measured for the second intrusion cycle.

have been examined. In order to define the composition of the reaction medium (expressed as molar ratios *versus* silica) a portion of wet monolith, coming from the phase separation in acidic medium and washed with water, was dried on paper, weighted, calcined at 550 °C for 8 h and weighed again to determine the amount of SiO_2 contained in the wet monolith preparation. In a typical synthesis (molar ratio: 1 SiO_2 : 0.3 CTAB : 0.2 NaOH : 400 H_2O), 0.342 g of a wet M2 monolith (82 mg calcined, 1.36 mmol SiO_2), 150 mg CTAB (0.408 mmol), 11.15 mg NaOH (0.273 mmol), and 9.8 mL H_2O (0.544 mol) were placed in a stainless autoclave and then maintained at 115 °C for 6 days. The monoliths were then washed with water, dried at 80 °C and calcined at 550 °C for 8 h.

Characterization

Powder X-ray diffraction (XRD) patterns were recorded on a Bruker AXS D8 diffractometer by using CuKα radiation and a Ni filter. The adsorption–desorption isotherms for nitrogen at 77 K were measured using a Micromeritics ASAP 2010 instrument on samples previously calcined at 550 °C in air for 8 h. Pore volumes are presented in volume of gas in the nitrogen isotherms and in volume of liquid in Table 2. Average pore diameters have been evaluated from the nitrogen desorption branch according to the Broekhoff and de Boer (BdB) method.[33,34] Examination of the particle morphology was achieved using a Hitachi S-4500 I scanning electron microscope (SEM). Transmission electron microscopy was performed on a 300 kV JEOL JEM-3010 instrument. Mercury porosimetry analysis was performed using a Micromeritics AutoPore IV 9500 Instrument on 100 mg of calcined monoliths. Samples were degassed at room temperature under vacuum. Pressures from 1 to 4000 bar were applied with an equilibrium time of 60 s at each pressure step.

Results and discussion

Preparation of the parent silica monoliths: formation of the macroporosity

All monoliths were obtained as white rods of 4 or 8 mm diameter and 4 or 8 cm length after calcination (Fig. 1). The size and shape of monoliths are determined by the size and shape of their initial molds ($(CH_3)_2SiCl_2$ hydrophobized glass tubes or PVC tubes). Initial molds had an internal diameter of 5 or 10 mm, corresponding to a total shrinkage of monoliths of 1 or 2 mm, respectively. Macropore and skeleton sizes can be controlled during the first step of silica monolith preparation in acidic media by inducing the phase separation of spinodal decomposition, where both the gel phase and the solvent phase are co-continuous, in parallel to the sol–gel transition in the alkoxy-derived sol–gel system. Different additives can be introduced to induce phase separation in the silica alkoxide–water system such as formamide,[22,35] polymers[22,23,36,37] or surfactants.[38,39] Nakanishi *et al.* have described this phenomenon very well in various publications.[22,23,35–39] The spinodal decomposition results from a change of the sign of the free energy of mixing in the system. The free energy ΔG_{mix}, which is negative at the beginning for the mixing of two components 1 and 2 becomes progressively positive; this is the driving force of the phase separation. The free energy of mixing is expressed by the Flory–Huggins formula (eqn (1)):[40–42]

$$\Delta G_{mix} = X_{12}\Phi_1\Phi_2 + RT([(\Phi_1/P_1)\ln \Phi_1 + (\Phi_2/P_2)\ln \Phi_2] = \Delta H_{mix} - T\Delta S_{mix} \quad (1)$$

where R is the ideal gas constant; T, the absolute temperature; Φ_i, the volume fraction of each component 1 and 2; P_i, the degree of polymerization of each component 1 and 2; X_{12}, the Flory–Huggins interaction parameter between components 1 and 2.

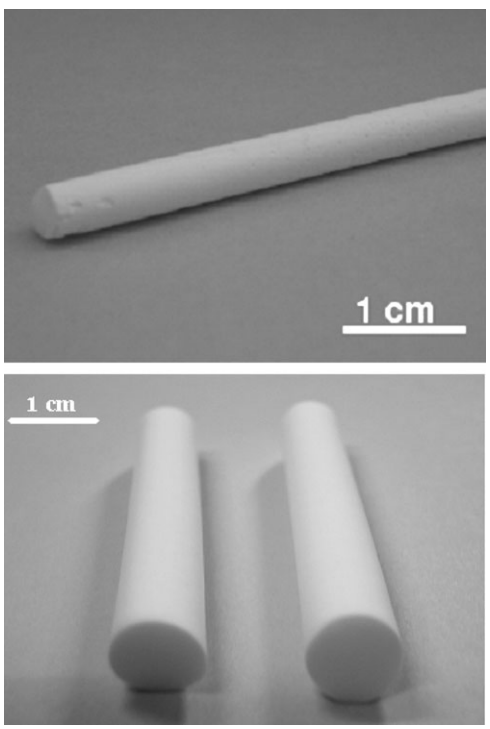

Fig. 1 Pictures of centimetre sized monoliths synthesized in this study.

The first term of eqn (1) represents the enthalpic contribution of the system:

$$\Delta H_{mix} = X_{12}\Phi_1\Phi_2$$

and the second term, the entropic contribution:

$$-\Delta S_{mix} = R[(\Phi_1/P_1)\ln \Phi_1 + (\Phi_2/P_2)\ln \Phi_2]$$

At the beginning of the process, the system is stable with a homogeneous mixture of the two components, which feature a negative ΔG_{mix}. When the gelification of the system starts, the degree of polymerization of silica increases and therefore the negative entropic term ($-\Delta S_{mix}$) decreases and ΔG_{mix} becomes less negative. The increase of the degree of polymerization of the silica leads to a less compatible mixture. The enthalpic term ΔH increases when the repulsive interaction between the two components increases. The polymerization of silica contributes also to the repulsion between the solvent and the silica phase. When ΔG_{mix} becomes positive, the phase separation occurs. To obtain a macroporous bicontinuous monolith, it is important that the phase separation be simultaneous with the sol–gel transition. If the gelification step is too slow and occurs after the phase separation, a separate dense silica phase will be obtained, while if the gelification is too fast and appears before the phase separation, a microporous dense silica will be obtained. If the two components consist only in a polymerizable silica precursor (alkoxides) and water, in an acidic medium the gelification is too fast and only a dense microporous silica phase is obtained. The use of additives (formamide, polymers, surfactants) is necessary to destabilize the initial system, *i.e.* to start with a less compatible initial mixture (silica–additive, water–additive) with a less negative free energy to allow the phase separation to be initiated just before the gelification. If the additive polymers are highly soluble in water (sodium polyacrylate, polystyrene sulfonate), the first component (water–polymer) exhibits weak interactions with the silica oligomers (second component), and the term X_{12} of eqn (1) and therefore ΔH_{mix} remains constant. In that case, the phase separation will be only induced by the polymerization of the silica, leading to a decrease of $-\Delta S_{mix}$. This mechanism is called the entropic system.

If the additives exhibit strong interactions (H-bonding) with the silica, the phase separation is induced by an enthalpic mechanism. The silica oligomers polymerize and at the same time are covered by polymers, which render silica less hydrophilic, increasing therefore the repulsive interaction between the first component (silica–polymer) and the second component (water). ΔH_{mix} increases and leads to the phase separation. The silica–polymer interaction should not be too strong however to avoid silica condensation. Organic polymers such as polyethylene oxide (PEO), poly(vinylpyrrolidone), polyacrylamide, or triblock copolymers such as $PEO_{20}PPO_{70}$-PEO_{20} are suitable to induce an enthalpic mechanism of phase separation with tetramethoxysilane or tetraethoxysilane (TEOS).[22,37] We have chosen to use polyethylene oxide (PEO) as the additive in our study. In the enthalpic driven system (interaction of polymers with silica), the phase separation and therefore the macropore size (water domain) can be controlled by different parameters: the amount of water, the amount of silica alkoxide, the amount of polymer and more precisely the number of ethylene oxide groups per silica (EO/Si), the polymer molecular weight and the temperature of the synthesis.

In the silica monolith synthesis using the system TEOS–PEO–H_2O–HNO_3, as in the present study, the size of the macropores of the silica monoliths has been adjusted in the range 2 to 20 μm, as observed by SEM (Fig. 2, Table 2), by varying the molecular weight of PEO from 10 000 to 100 000 g mol^{-1}, respectively. For a constant ratio EO/Si, the increase of the polymer molecular weight does not affect the enthalpy but leads to a decrease of the entropy and therefore to a lower initial negative free energy in the system. Thus, the phase separation is favored, resulting in the formation of larger macropores before the gelification. By mercury porosimetry (Fig. 3), it is possible to evaluate the macropore volume of the sample (Table 2) and the macropore size distribution by using

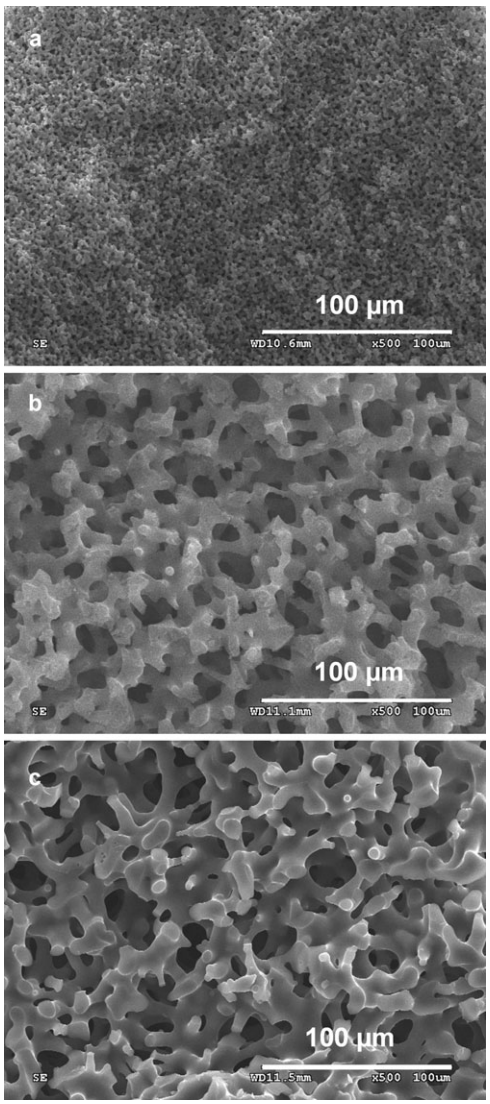

Fig. 2 SEM pictures of monoliths (a) M2, (b) M10, (c) M20 prepared by spinodal decomposition using different PEO polymers (M_w = 10 000, 35 000, 100 000), featuring macropores of 2, 10 and 20 μm, respectively.

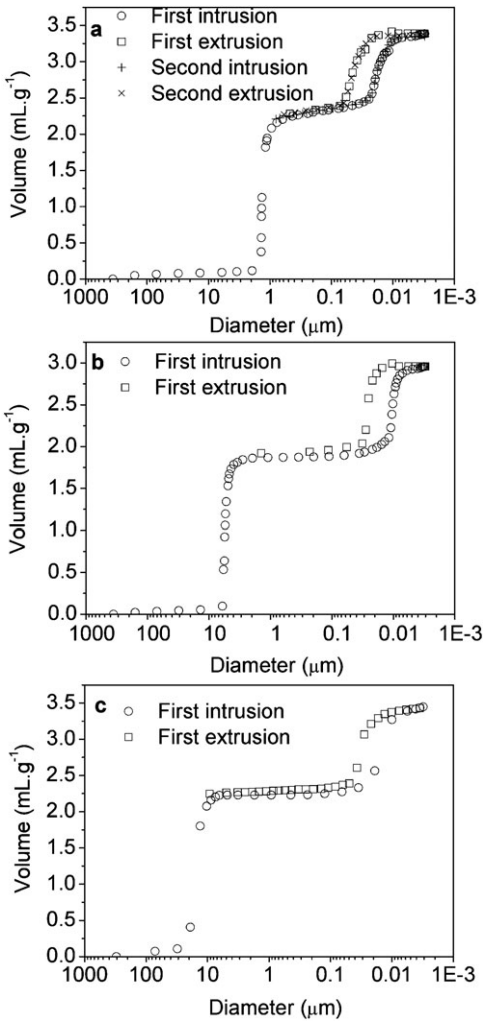

Fig. 3 Mercury porosimetry of monoliths (a) M2, (b) M10, (c) M20 prepared by spinodal decomposition and post-treated with ammonia solution to create a disordered mesoporosity inside the silica skeleton.

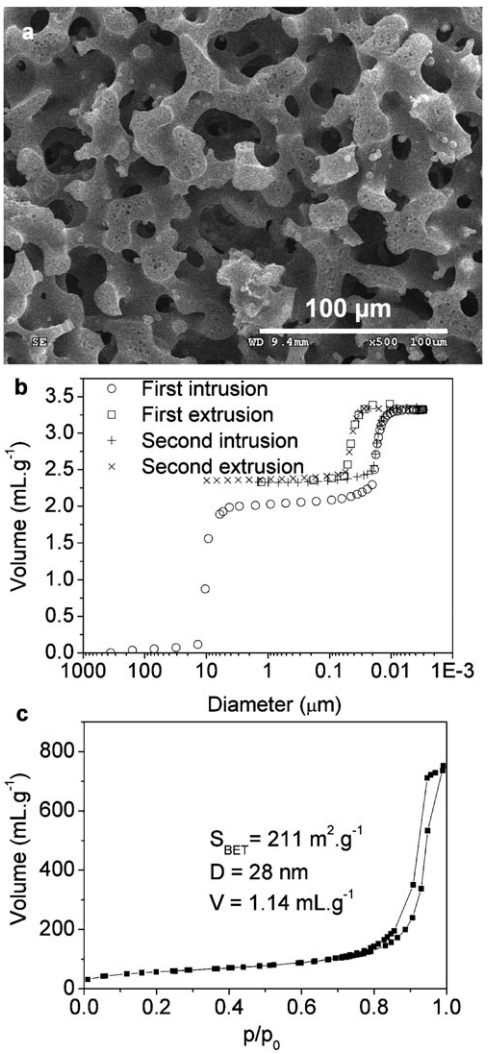

Fig. 4 (a) SEM, (b) mercury porosimetry and (c) nitrogen sorption isotherm at 77 K of monolith M15 post-treated with 1 M ammonia solution, featuring macropores of 15 μm and additional cavities of 1 μm in the silica skeleton.

the Laplace–Washburn equation (eqn (2)). Mercury penetrates into the pore of diameter (D) under a pressure (p) with a meniscus showing an advancing contact angle Θ between Hg and the solid surface. In mercury porosimetry, pore sizes instead of pressures are plotted *vs.* volume for an easier reading. The Laplace–Washburn equation has been established for uniform independent cylindrical pores, which is surely not the case for the present monoliths as evidenced by SEM in Fig. 2, but nevertheless, if we take a contact angle value of 130°, as is usually done, we can obtain an estimate of the average pore diameter and more importantly an evaluation of the pore size distribution, which is very difficult to obtain by analyzing SEM images. The Laplace–Washburn equation is as follows:

$$D = (-4\sigma \cos \Theta)/p \qquad (2)$$

with D being the pore size, p the intrusion pressure, Θ the contact angle between Hg and the solid surface and σ the Hg surface tension.

Mercury porosimetry of monoliths (Fig. 3) reveals two intrusion steps: one in the domain of micrometre-range macropores and one in the domain of nanometre-range mesopores. Indeed, mercury porosimetry has been performed on monoliths after acidic and basic post-treatment. This additional basic treatment induces formation of an additional mesoporosity, as explained in the following paragraph, and above all, brings to a higher stability to resist the pressure applied during the mercury intrusion (4000 bar). The very sharp step of mercury intrusion observed in the micrometre domains demonstrates the very uniform size of the macropores resulting from the phase separation process. Monoliths M2, M10 and M20 (Fig. 3) exhibit macropore sizes centered at 1, 5 and 16 μm and macropores volume of 2.1, 1.8, 2.1 mL g^{-1} (Table 2), respectively. Monolith M15, obtained under conditions similar to those engaged for the preparation of monolith M2 but with a lower amount of PEO (EO/Si = 0.580 instead of 0.593) features macropores of 9 μm in size (Fig. 4), as expected from the lower EO/Si molar ratio,[22] and a macropore volume of 1.9 mL g^{-1}. This sample presents also some cavities of 1 μm in its skeleton (visible by SEM) resulting from a second phase

separation occurring inside the silica skeleton. Mercury porosimetry reveals that these cavities of 1 μm are mainly located inside the skeleton, even if some cavities are visible on the surface by SEM, and do not interfere during macropore size or macropore volume determinations since no step in the intrusion branch is observed between 10 μm and 150 nm (Fig. 4b). These 1 μm cavities are filled by mercury after or during the mesopore filling. The majority of these 1 μm cavities are therefore connected to the macroporous network *via* the mesopores. After the intrusion, mercury is trapped in these cavities and can not be extruded; mercury extrusion in the mesopore domains shows an irreversibility of the total mesopore volume. The second intrusion cycle gives the real mesopore volume (around 1 mL g^{-1}) in accordance with the mesopore volume determined by nitrogen adsorption isotherm (Table 2, Fig. 4c). By difference the macropore volume developed by these 1 μm captive cavities is estimated at 0.35 mL g^{-1}.

Comments on the difference of macropore size determination by SEM and Hg porosimetry

It is noticeable that SEM pictures (Fig. 2 and Fig. 4) systematically indicate slightly larger macropore sizes than those calculated by the Laplace–Washburn equation from mercury porosimetry (Fig. 3 and Fig. 4b). By SEM, monoliths M2, M10, M15 and M20 feature macropore sizes of 2, 10, 15 and 20 μm, respectively, whereas mercury porosimetry results obtained by using the Laplace–Washburn equation with a classical contact angle of 130° leads to macropore size values of 1, 5, 9 and 16 μm (Table 2), respectively. This underestimation of the macropore sizes by mercury porosimetry measurements could be explained by considering that the Laplace–Washburn equation has been established for uniform straight non-connected cylindrical pores, using a constant contact angle between mercury and the solid surface. However, even if the macropore size distribution of the monoliths is narrow and the pores uniform, as confirmed by the very sharp steep step in the mercury intrusion branch, the macropores are clearly interconnected as imaged by SEM. The connections between the pores necessarily lead to a variation of the contact angle and the pressure has to be raised when the advancing meniscus enters a connection. This behavior is believed to be the origin of the difference between macropore sizes measurement by SEM and Hg porosimetry. A similar observation, and conclusion, has been reported in the determination of the size of macropores of chromatography monoliths using laser scanning confocal microscopy.[43]

The underestimation of pore sizes obtained by Hg porosimetry has also been noticed in the case of mesopore size determinations of SBA-15 materials presenting some connections between the channels when comparing the results obtained by mercury porosimetry and nitrogen sorption.[44]

Stabilization of the monolith and generation of disordered mesopores by secondary treatment

Monoliths obtained after the first acidic treatment were submitted to an ammonia hydrothermal post-treatment to stabilize them, which at the same time induces the formation of a disordered mesoporosity. After the first acidic step monoliths show a very low condensation state of silica with only 30% of Q_4 ($Si(OSi)_4$) by ^{29}Si MAS NMR[25] and could not resist the pressure applied during mercury porosimetry measurements (until 4000 bar). The ammonia basic treatment promotes the condensation of the silanol groups up to a value of Q_4 = 70% and so leads to a stabilization of the monolith skeleton. The high mechanical stability of the skeleton is evidenced by the identical mesopore volumes reached upon intrusion and extrusion and, above all, by the superposition of the second intrusion–extrusion cycle over the first one in mercury porosimetry (Fig. 3). This shows that the textural characteristics (macro and mesoporosity) were not altered after mercury intrusion at 4000 bar. The fact that the extrusion branch parallels the intrusion branch also confirms this result. The mesoporosity network created inside the silica skeleton by the basic post-treatment results from a dissolution–reprecipitation process of the silica network without changing the morphology of the bi-continuous system of macropores and silica. This is an example of pseudomorphic transformation where the structural and textural features of a solid are modified without changing the morphology of the parent system. Under ammoniacal treatment, the silica skeleton condenses into nanoparticles giving rise to a disordered interparticular mesoporosity. The size of the mesopores is controlled by the temperature of the basic treatment[25] or, as in the present study, by the concentration of ammonia for a given temperature. At 80 °C, mesopores of around 20, 25, 30 nm have been obtained for ammonia concentrations of 0.1, 0.5 and 1 M, respectively (Table 1 and Table 2). These changes arise from the formation of larger nanoparticles inside the skeleton for higher ammonia concentration and, as a consequence, lead to lower surface areas (500, 250, 200 m^2 g^{-1}, respectively).

The adsorption and desorption branches of the nitrogen isotherms (Fig. 4c and Fig. 5) and the two branches of intrusion and extrusion of the mercury isotherms are vertical (Fig. 3 and Fig. 4b), which suggests that the distribution of the sizes of the mesopores is uniform. It has to be noticed that for extrusion, the Laplace–Washburn equation should not be applied directly because the mechanism for emptying the pore is different from that of pore filling, which is at the origin of the observed hysteresis cycle.[43] Nevertheless, the same remark concerning the underestimation of macropore sizes by mercury porosimetry can be made for the evaluation of the mesopore size by comparing the position of the second step in the mercury intrusion (Fig. 3 and Fig. 4b) with the values of mesopore diameters obtained from the nitrogen desorption isotherm (Fig. 4c and Fig. 5) (Table 2). The interparticular mesoporosity developed in the monoliths is also an interconnected porosity and the Laplace–Washburn assumption of straight independent pores and constant contact angle is, again, not fulfilled.

Preparation of MCM-41 monoliths by pseudomorphic transformation

The main goal of this study was to examine the possibility of transforming the unstructured mesoporosity of the monolith skeleton into an ordered structured mesoporosity of MCM-41

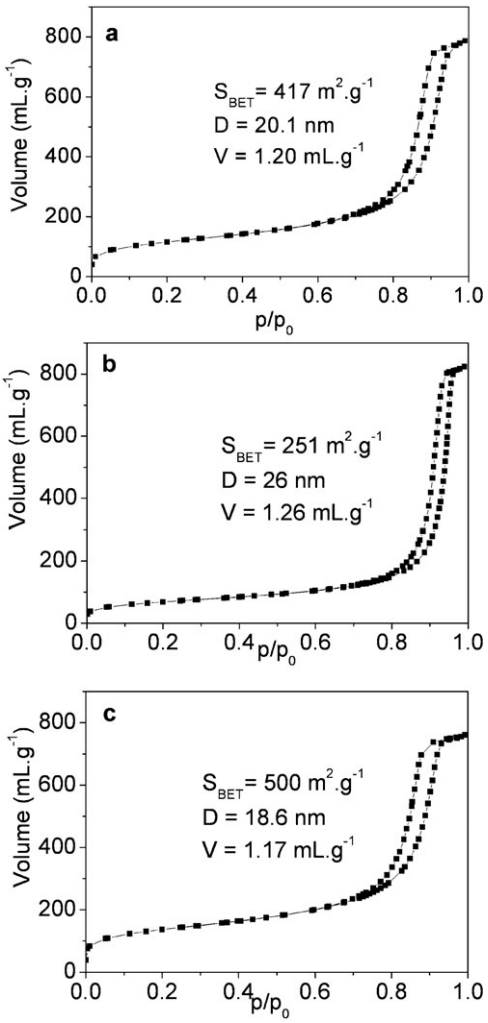

Fig. 5 Nitrogen sorption isotherms at 77 K of monoliths (a) M2, (b) M10, (c) M20 prepared by spinodal decomposition and post-treated with 0.1, 0.5 and 0.1 M ammonia solutions, respectively. Generation of a disordered mesoporosity around 20 nm in the silica skeleton.

type by pseudomorphic transformation. This means maintaining architectures of the silica skeleton and of the macroporosity while transforming the mesoporous network of the skeleton into an ordered one. Such a process should allow one to obtain an independent control of the macroporosity and of the mesoporosity, which was not the case in the previous studies.[26–30]

The pseudomorphic transformation is a synthesis strategy we developed since 2002 to control the particle morphology of micelle-templated silicas (MTS such as MCM-41 and MCM-48) at the micro- to milli-metre scale, a key step for incorporating these materials into applicable systems. Pseudomorphic transformation of a disordered mesoporosity into an ordered one has been successfully applied to spherical silica particles of 5, 10, 50 μm and 1 mm diameter.[31,32] Pseudomorphism is well known in the mineral world. It allows preparation of a mineral with a morphology not related to its crystallographic symmetry group. The resulting mineral takes the outward crystal habit of a different mineral. This transformation occurs at a non-constant matter content, by using a mineralization solution that exchanges anions (or cations) with an existing (pre-shaped) solid body and allows the new structure to precipitate while maintaining the existing morphology. The concept of pseudomorphic transformation was applied to amorphous pre-shaped silica particles to produce MTS with the same morphology, using alkaline solution to dissolve the silica and re-precipitate it around CTAB surfactant micelles into the ordered MTS structures, all of this process occurring inside the particle. MTS with hexagonal and cubic symmetry and different pore sizes and control morphology have been synthesized. The new pseudomorphs have been successfully used as chromatography supports, a very demanding application in terms of particle size and morphology. This pseudomorphic transformation has never been applied to larger, eye-visible objects of centimetre scale, such as monolithic pieces.

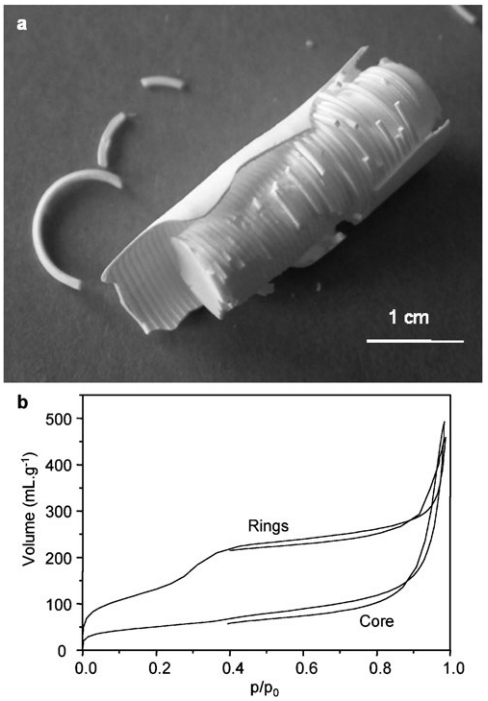

Fig. 6 (a) Picture of the material obtained after pseudomorphic transformation performed on a calcined monolith and (b) nitrogen sorption isotherm at 77 K of the outer rings and of the inner core of the solid.

The first attempts of pseudomorphic transformation were performed on calcined mesoporous/macroporous silica monoliths of 8 mm diameter and 4 cm length prepared according to the complete Nakanishi synthesis procedure, in other words after the secondary ammoniacal treatment and a calcination at 550 °C. The monoliths were reacted in basic CTAB solutions with a composition corresponding to that established earlier for the transformation of amorphous spherical silica particles into MCM-41 (1 SiO_2–0.1 CTAB–0.1 NaOH–130 H_2O). This approach led to only a partial transformation of the monolith and to a loss of its original morphology (Fig. 6a). The resulting material appeared as a shell and rings composed mostly of MCM-41, as evidenced by the nitrogen sorption isotherm, and a core of mesoporous silica with a very large pore size (Fig. 6b). The peculiar shape of the MCM-41-rich phase is typical for the growth of hexagonal silica under low pH or

dilute quiescent conditions.[45,46] These conditions favour the formation of fibers which evolve upon growing into gyroid or curved shapes due to the formation of topological defects. Although the reaction was performed under alkaline conditions it can be considered that a slow dissolution rate of the silica of the monolith skeleton, due to its previous calcination, associated with a fast precipitation of the MCM-41 phase could account for a growth mechanism similar to that proposed in acidic medium. A stable MCM-41 material would form in the surface of the monolith in contact with the basic solution as soon as some silicates become available in the solution. Once the surface is covered with MCM-41, further diffusion and exchange between the skeleton mesopores and the CTAB solution is limited, or prevented, and the process of pseudomorphic transformation is blocked. The MCM-41 nuclei grow under dilute conditions and develop the peculiar ring shape, distinct from that of the original monolith skeleton.

The above limitation could be overcome by performing the pseudomorphic transformation on silica monoliths obtained after the first step, in acidic medium, where the degree of silica condensation is very low. Different monoliths with varying macropore and skeleton sizes have been used to illustrate the potential of the procedure. Wet silica monoliths coming from the first acidic step, washed with water and dried on paper, were immersed in a basic solution of CTAB micelles and reacted in an autoclave. Different parameters were explored, among them the amount of NaOH, of CTAB and of water. The hydrothermal conditions of the transformation were set at 115 °C for 6 days, which correspond to the conditions previously determined for the complete pseudomorphic transformation of spherical silica particles into MCM-41.

The variation of the NaOH amount from 0.05 < NaOH < 0.20 in the system of molar ratio: 1 SiO_2–0.2 CTAB–x NaOH–100 H_2O, reveals that the stable (no cracks) monoliths consisting of pure MCM-41 are obtained up to an amount of NaOH of 0.15. For a NaOH content of 0.20, the monolith presents some cracks. Nitrogen sorption isotherms of calcined monoliths reveal that the sharp step at $p/p_0 = 0.35$ characteristic of the presence of uniform mesopores of 3.5 nm (typical of MCM-41 mesoporosity) becomes apparent after treatment with a concentration ratio of NaOH of 0.09 (Fig. 7a). By XRD (Fig. 7b), the peaks characteristic of the ordering of the mesopores of MCM-41 appear after a reaction with a NaOH amount equal to $x = 0.13$ which indicates the formation of larger domains of MCM-41. The highest degree of ordering is obtained for a NaOH molar ratio of $x = 0.15$. The XRD pattern of the material features a d-spacing of 4.0 nm and a bump around 4° in 2θ corresponding to the position of the other orders of MCM-41 type materials. The pseudomorphic transformation has allowed maintaining the architecture of the macroporosity and the morphology of the silica skeleton as shown by the SEM pictures (Fig. 7c). This monolith synthesized by applying a secondary treatment with a solution of molar composition 1 SiO_2–0.2 CTAB–0.15 NaOH–100 H_2O features a distribution of macropores and a silica skeleton identical to the monoliths disclosed by Nakanishi with, in addition, a structured mesoporosity with a pore volume of 0.55 mL g^{-1}, a surface area of 730 m^2 g^{-1} and pore size of 3.5 nm.

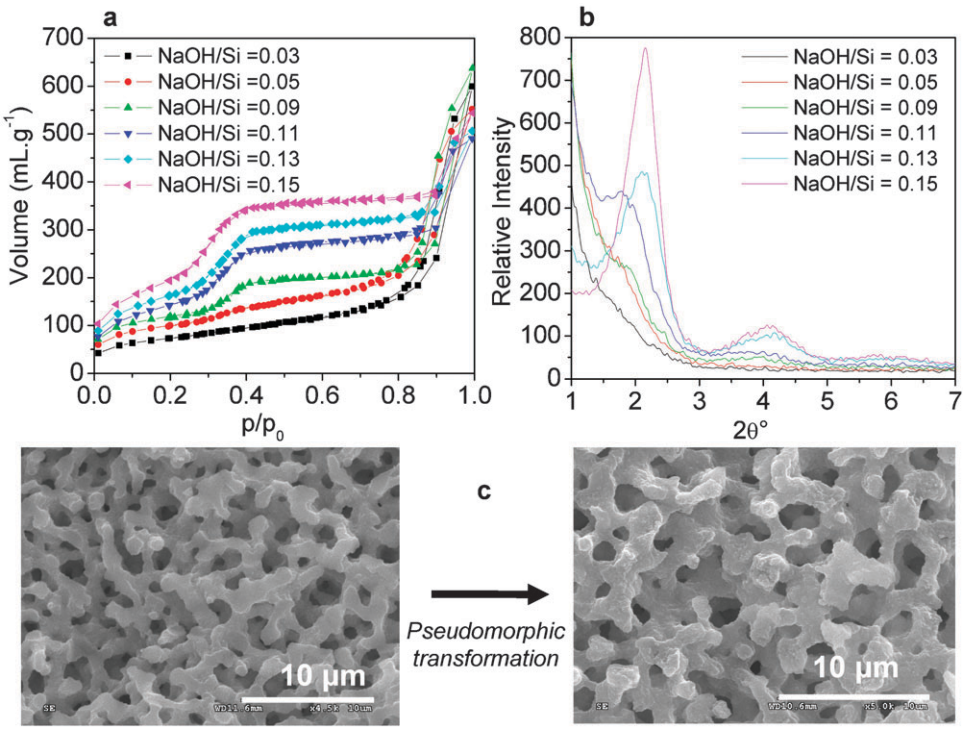

Fig. 7 (a) Nitrogen sorption isotherm at 77 K and (b) XRD pattern of M2 monoliths after pseudomorphic transformation for the system of molar composition 1 SiO_2–0.2 CTAB–x NaOH–100 H_2O, with $0.05 < x < 0.15$; and (c) SEM pictures of monoliths before and after pseudomorphic transformation with $x = 0.15$.

Optimization of the synthesis of MCM-41 monoliths

In the material described above, however, a second network of large mesopores, evidenced in the nitrogen isotherms at values of p/p_0 higher than 0.9, persists after the pseudomorphic transformation due to interparticular voids inside the silica skeleton. This secondary mesoporosity arises from an incomplete transformation of the whole silica skeleton into MCM-41, as previously observed for the pseudomorphic transformation of spherical particles.[31] In that case, complete transformation, and disappearance of the secondary large mesoporosity, was achieved either by increasing the reaction time (up to 6–7 days), or by forming an MCM-41 phase with a higher pore volume. In the case of monoliths, applying longer synthesis times (up to 12 days) did not allow elimination of the extra mesoporosity. Formation of an MCM-41 material with a larger pore volume was therefore attempted. In classical MCM-41 synthesis, higher pore volumes may be obtained by either increasing the CTAB or the NaOH amounts. In both cases, wall thickness of the material is reduced.

Increasing the CTAB amount in a system of molar ratio 1 SiO_2–x CTAB–0.15 NaOH–100 H_2O, with $0.05 < x < 0.5$, results effectively in an increase of the pore volume (Fig. 8a) in the range $0.05 < x < 0.2$. The pore volume remains nearly the same for higher CTAB amounts. Sharper XRD peaks (Fig. 8b) are obtained for a CTAB ratio $x = 0.3$ revealing a slightly better ordering of the MCM-41 network for this composition. However, the second mesoporosity is still observable.

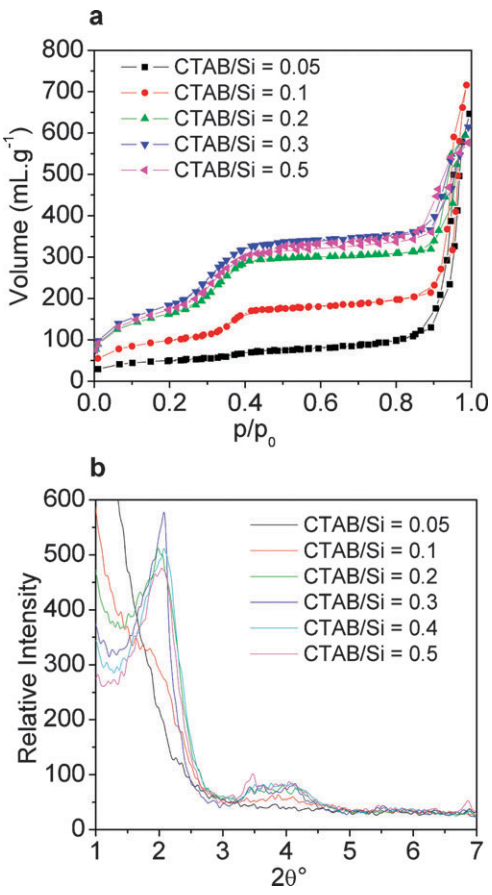

Fig. 8 (a) Nitrogen sorption isotherm at 77 K and (b) XRD patterns of M2 monoliths after pseudomorphic transformation for the system of molar composition 1 SiO_2–x CTAB–0.15 NaOH–100 H_2O, with $0.05 < x < 0.50$.

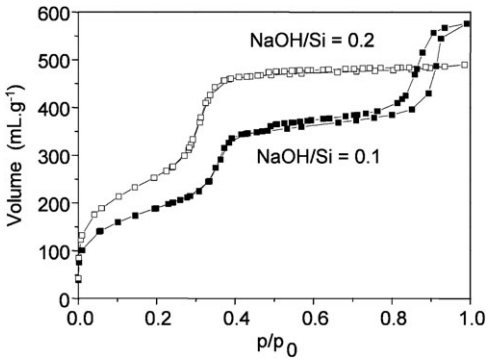

Fig. 9 Nitrogen sorption isotherm at 77 K of M15 monoliths after pseudomorphic transformation for the system of molar composition 1 SiO_2–0.3 CTAB–x NaOH–400 H_2O, with $0.1 < x < 0.2$.

The second alternative is to increase the amount of NaOH, a parameter which should be used cautiously however to avoid the appearance of cracks in the monolith (see above) due to too fast a transformation. In order to increase the NaOH amount while reducing the rate of the pseudomorphic transformation a higher dilution was used. Increasing the amount of NaOH in a more dilute system, corresponding to a molar composition 1 SiO_2–0.3 CTAB–x NaOH–400 H_2O, with $0.1 < x < 0.2$, avoided the formation of cracks in the monolith and, for $x = 0.2$, allowed full elimination of the second mesoporosity (Fig. 9). The MCM-41 materials obtained at $x = 0.1$ and 0.2 exhibited pore volumes and surface areas of 0.53 to 0.72 mL g^{-1} and 690 to 950 m^2 g^{-1}, respectively and the typical ordering of the mesopores as evidenced by XRD and TEM (Fig. 10).

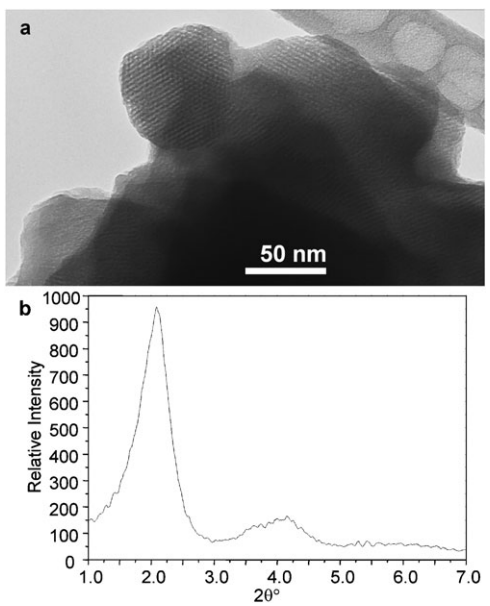

Fig. 10 (a) TEM and (b) XRD of M15 monoliths after pseudomorphic transformation for the system of molar ratio 1 SiO_2–0.3 CTAB–0.2 NaOH–400 H_2O.

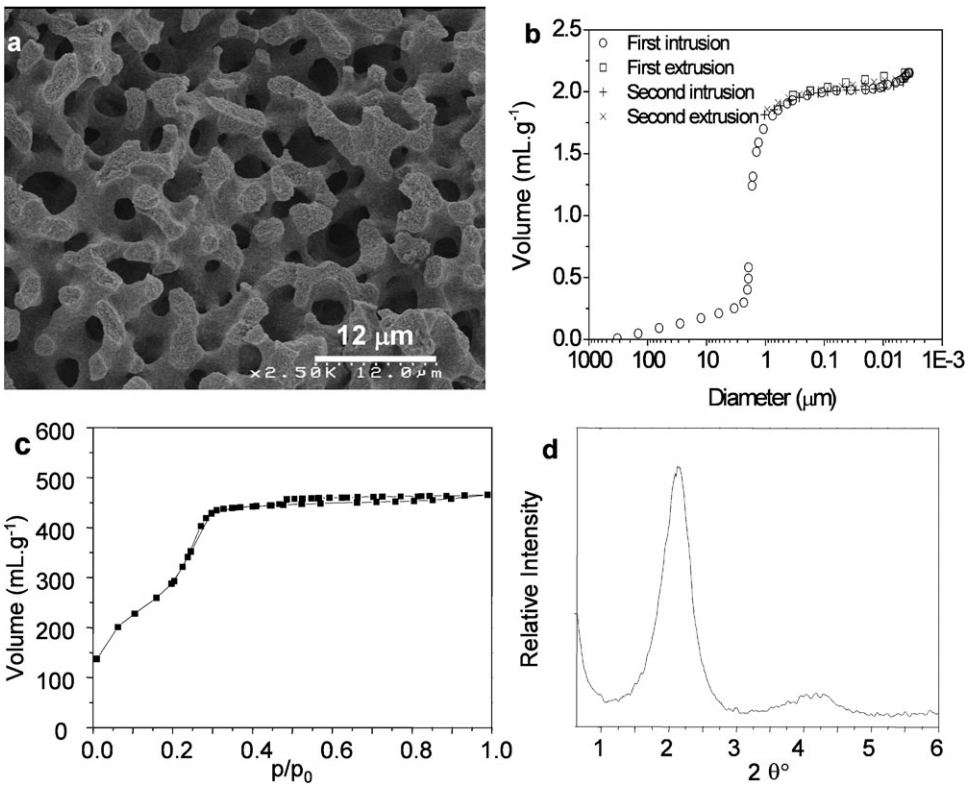

Fig. 11 Characteristics of an M2 monolith after pseudomorphic transformation performed under optimized conditions (1 SiO_2–0.3 CTAB–0.2 NaOH–400 H_2O) (a) SEM image of the silica skeleton, (b) mercury porosimetry, (c) nitrogen sorption isotherm at 77 K and (d) XRD pattern.

Monoliths with different macroporosity have been then treated under these optimized experimental conditions (1 SiO_2–0.3 CTAB–0.2 NaOH–400 H_2O), demonstrating that independent control of the macroporosity and the generation of an ordered mesoporosity can be gained by the pseudomorphic procedure. The previous study was illustrated with a monolith featuring 15 µm macroporosity (Fig. 9 and Fig. 10). An example of pseudomorphic transformation of a monolith featuring 2 µm macroporosity is presented in Fig. 11. Mercury porosimetry, SEM, nitrogen adsorption and XRD reveal the pseudomorphic transformation of the skeleton into an MCM-41 type distribution of pores (Fig. 11). No extra mesoporosity is formed by this process as confirmed by mercury porosimetry featuring only the macroporosity of the monolith (too high a pressure would be needed to fill MCM-41 pores, which are not visible by mercury intrusion). Pseudomorphic transformation therefore proves a versatile technique, which can be applied even to macroscopic objects.

Conclusion

Suitable conditions have been found to reach independent control of the macroporosity and the ordered mesoporosity of the MCM-41 type of silica monoliths by pseudomorphic transformation. This was possible by generating first the macroporosity and the skeleton of the monolith by spinodal decomposition between a silica rich phase and a water rich phase in acidic medium and then by applying a pseudomorphic synthesis procedure to this low condensed silica skeleton with a basic solution containing surfactant micelles. Rods of 4 or 8 cm length and 4–8 mm diameter have been obtained. Monoliths with 1–2 µm macropores will be further tested in separation processes and compared with commercial monoliths (Chromolith, from Merck) to study the influence of an ordered porosity in chromatography applications, as we have previously done for spherical particles.[25,31] Monoliths with larger macroporosity (>10 µm) will be used in catalytic applications for reactions such as selective hydrogenation or oxidation, involving very short contact times.

Acknowledgements

The authors thank TOTAL S.A. for financial support.

References

1 A. Galarneau, F. Di Renzo, F. Fajula, L. Mollo, B. Fubini and M. F. Ottaviani, *J. Colloid Interface Sci.*, 1998, **201**, 105.
2 M. F. Ottaviani, A. Moscatelli, D. Desplantier-Giscard, F. Di Renzo, P. J. Kooyman, B. Alonso and A. Galarneau, *J. Phys. Chem. B*, 2004, **108**, 12123.
3 M. F. Ottaviani, A. Galarneau, D. Desplantier-Giscard, F. Di Renzo and F. Fajula, *Microporous Mesoporous Mater.*, 2001, **44**, 1.
4 F. Di Renzo, A. Galarneau, P. Trens and F. Fajula, *Handbook of Porous Materials*, Wiley-VCH, Weinheim, 2002.
5 Q. Sun, E. G. Vrieling, R. A. van Santen and N. A. J. M. Sommerdijk, *Curr. Opin. Solid State Mater. Sci.*, 2004, **8**, 111.
6 D. Zhao, P. Yang, Q. Huo, B. F. Chmelka and G. D. Stucky, *Curr. Opin. Solid State Mater. Sci.*, 1998, **3**, 111.
7 J. S. Beck, J. C. Vartuli, W. J. Roth, M. E. Leonowicz, C. T. Kresge, K. D. Schmitt, C. T.-W. Chu, D. H. Olson, E. W. Sheppard, S. B. McCullen, J. B. Higgins and J. L. Schlenker, *J. Am. Chem. Soc.*, 1992, **114**, 10834.
8 A. Corma, *Chem. Rev.*, 1995, **95**, 559.

9 A. Taguchi and F. Schüth, *Microporous Mesoporous Mater*., 2004, **77**, 1.
10 J. Kim, J. W. Grate and P. Wang, *Chem. Eng. Sci*., 2006, **61**, 1017.
11 H. H. P. Yiu and P. A. Wright, *J. Mater. Chem*., 2005, **15**, 3690.
12 M. Ogawa, *J. Photochem. Photobiol., C*, 2002, **3**, 129.
13 C. Charnay, S. Begu, C. Tourne-Peteilh, L. Nicole, D. A. Lerner and J. M. Devoisselle, *Eur. J. Pharm. Biopharm*., 2004, **57**, 533.
14 M. Antonietti, B. Berton, C. Goltner and H. P. Hentze, *Adv. Mater*., 1998, **10**, 154.
15 B. Lebeau, C. E. Fowler, M. S. C. Farcet, B. Charleux and C. Sanchez, *J. Mater. Chem*., 2000, **10**, 2105.
16 K. H. Rhodes, S. A. Davis, F. Caruso, B. J. Zhang and S. Mann, *Chem. Mater*., 2000, **12**, 2832.
17 J. S. Yin and Z. L. Wang, *Appl. Phys. Lett*., 1999, **74**, 2629.
18 L.-Y. Xu, Z. Shi and Y.-Q. Feng, *Microporous Mesoporous Mater*., 2007, **98**, 303.
19 P. Schmidt-Winkel, W. W. Lukens, P. D. Yang, D. I. Margolese, J. S. Lettow, J. Y. Ying and G. D. Stucky, *Chem. Mater*., 2000, **12**, 686.
20 S. A. Bagshaw, *Chem. Commun*., 19999), 767.
21 B. J. Zhang, S. A. Davis and S. Mann, *Chem. Mater*., 2002, **14**, 1369.
22 K. Nakanishi, *J. Porous Mater*., 1997, **4**, 67.
23 K. Nakanishi and N. Soga, *J. Non-Cryst. Solids*, 1992, **139**, 1.
24 K. Nakanishi, H. Shikata, N. Ishizuka, N. Koheiya and N. Soga, *J. High Resolut. Chromatogr*., 2000, **23**, 106.
25 A. Galarneau, J. Iapichella, D. Brunel, F. Fajula, Z. Bayram-Hahn, K. Unger, G. Puy, C. Demesmay and J.-L. Rocca, *J. Sep. Sci*., 2006, **29**, 844.
26 N. Huesing, C. Raab, V. Torma, A. Roig and H. Peterlik, *Chem. Mater*., 2003, **15**, 2690.
27 T. Amatani, K. Nakanishi, K. Hirao and T. Kodaira, *Chem. Mater*., 2005, **17**, 2114.
28 K. Nakanishi, Y. Kobayashi, T. Amatani, K. Hirao and T. Kodaira, *Chem. Mater*., 2004, **16**, 3652.
29 Z.-G. Shi, Y.-Q. Feng, L. Xu and D. S. L. and Y. Y. Ren, *Microporous Mesoporous Mater*., 2004, **68**, 55.
30 J.-H. Smatt, S. Schunk and M. Linden, *Chem. Mater*., 2003, **15**, 2354.
31 A. Galarneau, J. Iapichella, K. Bonhomme, F. Di Renzo, P. Kooyman, O. Terasaki and F. Fajula, *Adv. Funct. Mater*., 2006, **16**, 1657.
32 T. Martin, A. Galarneau, F. Di Renzo, F. Fajula and D. Plee, *Angew. Chem., Int. Ed*., 2002, **41**, 2590.
33 J. C. P. Broekhoff and J. H. De boer, *J. Catal*., 1968, **10**, 377.
34 A. Galarneau, D. Desplantier, R. Dutartre and F. Di Renzo, *Microporous Mesoporous Mater*., 1999, **27**, 297.
35 H. Kaji, K. Nakanishi and N. Soga, *J. Non-Cryst. Solids*, 1995, **185**, 18.
36 K. Nakanishi and N. Soga, *J. Am. Chem. Soc*., 1991, **74**, 2518.
37 K. Nakanishi, H. Komura, R. Takahashi and N. Soga, *Bull. Chem. Soc. Jpn*., 1994, **67**, 1327.
38 Y. Sato, K. Nakanishi, K. Hirao, H. Jinnai, M. Shibayama, Y. B. Melnichenko and G. D. Wignall, *Colloids Surf., A*, 2001, **187**, 117.
39 K. Nakanishi, Y. Sato, Y. Ruyat and K. Hirao, *J. Non-Cryst. Solids*, 2003, **26**, 567.
40 P. J. Flory, *J. Chem. Phys*., 1942, **10**, 51.
41 M. Huggins, *J. Phys. Chem*., 1942, **46**, 151.
42 M. Huggins, *J. Am. Chem. Soc*., 1942, **64**, 1712.
43 H. Saito, K. Nakanishi, K. Hirao and H. Jinnai, *J. Chromatogr., A*, 2006, **28**, 95.
44 A. Galarneau, B. Lefevre, H. Cambon, B. Coasne, S. Valange, Z. Gabellica, J.-P. Bellat and F. Di Renzo, *J. Phys. Chem. C*, 2007, submitted.
45 G. A. Ozin, C. T. Kresge and H. Yang, *Adv. Mater*., 1998, **10**, 883.
46 S. M. Yang, H. Yang, N. Coombs, I. Sokolov, C. T. Kresge and G. A. Ozin, *Adv. Mater*., 1999, **11**, 52.